3D Model-based Reconstruction of the Proximal Femur from Low-dose Biplanar X-Ray Images

Haithem Boussaid[1,2]
haithem.boussaid@ecp.fr
Samuel Kadoury[5]
samuel.kadoury@philips.com
Iasonas Kokkinos[1,2]
iasonas.kokkinos@ecp.fr
Jean-Yves Lazennec[4]
lazennec.jy@wanadoo.fr
Guoyan Zheng[3]
Guoyan.Zheng@istb.unibe.ch
Nikos Paragios[1,2]
nikos.paragios@ecp.fr

[1] Center for Visual Computing
Ecole Centrale Paris, France
[2] Equipe GALEN, INRIA Saclay
Île de France, Orsay, France
[3] Institute for Surgical Technology and Biomechanics
University of Bern, Switzerland
[4] Centre Hospitalier Universitaire Pitié Salpétrière, Paris, France
[5] Philips Research North America
345 Scarborough Rd
Briarcliff Manor, NY, 10510 USA

Abstract

The 3D modeling of the proximal femur is a valuable diagnostic tool for orthopedic surgery planning. The use of computed tomography is the most prominent modality to visualize bones both in terms of resolution as well as in term of bone/tissue separation. Towards reducing the impact of radiation to the patient, low-dose X-ray imaging systems have been introduced while still providing partial views with rather low signal-to-noise ratio. In this paper, we focus on automating the 3D proximal femur reconstruction from simultaneously acquired 2D views. A deformable model represented by triangulated mesh surfaces extends to a linear sub-space describing the variations across individuals. Segmentation consists of inferring a global deformation of 3D model followed by a local adaption based on the most prominent combination of the sub-space parameters. The basis of which relies on the minimization of a cost function based on the biplanar projection of this model. To this end, we employ an active region model that aims at optimizing the 3D model parameters such that projection of surface is attracted from edge potentials, while creating an optimal partition between the bone class and the remaining structures. The global parameters of the model and the local ones are optimized through a gradient-free approach. Promising results demonstrate the potentials of our method compared to a supervised reconstruction technique.

1 Introduction

Personalized 3D proximal femur planning inherits important diagnostic interest in related surgical interventions such as total hip replacement and intertrochanteric osteotomy [3].

BMVC 2011 http://dx.doi.org/10.5244/C.25.35

Conventional 3D imaging modalities such as CT and MRI have been the standard of care for these types of applications. However, CT induces high radiation doses to the patient while MRI cannot be performed for follow-up cases with post-operative metallic implants. Moreover, these modalities require the patient to be lying down, causing a long acquisition protocol with a clinically insignificant patient positioning to assess physiological function. In order to reduce radiation, prior works have focused on 3D reconstruction methods from bi-planar X-ray images based on stereovision techniques [5, 13]. Our work lies within this scope using the low dose EOS imaging system (*BiospaceMed*^{TM}) which is an alternative modality producing simultaneous biplanar X-ray images in an upright position.

Since 3D shape reconstruction from only biplane images is a fundamentally challenging problem, the alternative is to use prior knowledge with regards to variability in structural changes, taking advantage from the fact that bones have their standard patterns of distribution [4]. In this paper, we seek to build a parametric model learned from a training set and automatically perform a 3D reconstruction of the proximal femur based on available 2D information from the patient's image. The problem is thus formulated as an adaptive 2D/3D registration.

Active shape models [1] elegantly describe the variation of a shape in a population and has been shown to accurately model anatomical objects. Another approach is to build a hybrid atlas [10] described by a set of connecting spheres contained within the bounding surface of the shape, thus creating a higher number of parameters to optimize.

Solving the 2D/3D registration problem has been extensively investigated in medical imaging and computer vision. In [6], the authors propose to segment the femur contours in the X-ray images through a level set technique in order to build a distance map before proceeding to registration. Feature-based registration techniques rely on identifying specific landmarks [7, 9] and thus require the user intervention and a suitable user interface which is not practical an in inter-operative context. Other approaches have attempted to solve the problem through digitally reconstructed X-rays (DRR) based techniques, which are time consuming with limited results. Since the main challenge of X-ray imaging is the low image quality with overlapping structures hindering the visibility of anatomical landmarks, the definition of a robust objective function as well as the optimization scheme is challenging.

In this paper, we consider an iconic approach to address the above mentioned limitations. Prior knowledge is represented in the 3D space using a linear 3D point-based subspace model that is learned from a training dataset. The inference is performed using an active region model that seeks silhouette/edge proximity with optimal regional separation of intensities between bones and the rest of the image. Using the projection matrix associated with this modality, and an optimization method that does not require the computation, we optimize the 3D model parameters using the information being observed in the X-ray images. We propose thus a one stage automatic framework that solves the problem of joint 3D reconstruction and 2D segmentation of the proximal femur.

2 Statistical Model Construction

2.1 Model parameters

The aim of building the parametric model is to use a training dataset of triangulated meshes from segmented CT to compute the principal components of shape variation from the patient population. Principal component analysis (PCA) is used to describe the different modes of

variation with a restricted number of parameters [1]. The axes of the shape space are oriented along directions in which the data has its highest variance (Fig. 1(a)). In order to compensate for the varying positioning during CT acquisition, we use a Demon's algorithm [11]to estimate the dense deformation fields between the binary volumes after a scaled rigid registration was applied. Each estimated deformation field is then used to displace the positions of the vertices of the reference surface model to the associated target volume. We thus obtain surface models with established point correspondences. As a scaled rigid registration is applied before the non-rigid registration for each model, our model only captures the shape variations but not the scales:

$$\widehat{S}(\mathbf{R},\mathbf{D}) = \overline{S}(\mathbf{R}) + \sum_{i=1}^{L} w_i V_i \tag{1}$$

where $\overline{S}$ is the mean shape. $\mathbf{R}$ is a vector describing the rigid parameters. In addition, $\mathbf{D} = \{w_i\}_{i=1}^{L}$ are the shape parameters which needs to be determined and $\{V_i\}_{i=1}^{L}$ are the eigenvectors.

2.2 Modeling the projection of the low-dose X-ray system

The EOS system is a radiographic imaging modality designed to dramatically reduce radiation doses using revolutionary particle detectors and an acquisition technique based on line-scanning. Because of these novel capabilities, EOS enables simultaneous acquisitions of two images, coronal and sagittal views in the upright position (Fig. 1(b)). Due to the particular fan beam projection, the system projection matrix does not follow the classical perspective model applied in stereovision theory. If $M(x,y,z)$ is a 3D point in the EOS cabin and $Pt(wu,v,w)$ its projection point in the reference plane, the projection matrix $\mathbf{M}$ is as follows:

$$\begin{pmatrix} wu - L_1 \\ v - L_2 \\ w - 1 \end{pmatrix} = \begin{pmatrix} 0 & \frac{SR}{SI} & 0 \\ 0 & 0 & 1 \\ \frac{-1}{SI} & 0 & 0 \end{pmatrix} \begin{pmatrix} x \\ y \\ z \end{pmatrix} \tag{2}$$

where $L1$ and $L2$ represent the translation parameters. Note that the coordinate v is not multiplied by w and no homothetic transformation is applied in z. SR is source reference plane distance and SI is the source isocenter distance.

2.3 Projection of the 3D silhouette contour

A crucial component of 2D/3D registration scheme is that available information is represented in different spaces. One of the key challenges is then the need for an appropriate way to compare multidimensional datasets (3D triangulated parametric model and bi-planar X-ray images). We extract the silhouette of the 3D model of the femur by projecting silhouette edges in 2D, with respect to the system projection matrix, allowing us to create a binary mask defining the region inside and outside of the femur and the contours naturally (Fig. 2). Because of the line-sweeping acquisition technique of the X-ray beams, our silhouette computation and definition is different from state of the art techniques. It consists of the mesh edges which are adjacent to both a front facing and a back facing polygon. A mesh polygon is front facing to a given point of view P if its plane equation is a positive multiplicative factor. Otherwise it is back facing. Note that P changes it's value along the Z axis during the acquisition.

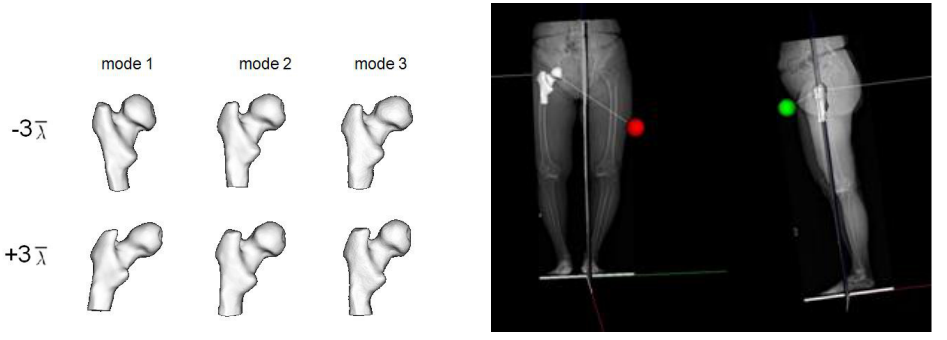

(a) (b)

Figure 1: (a) The first two eigenmodes of variation of the model and (b) the geometrical setup of the EOS system.

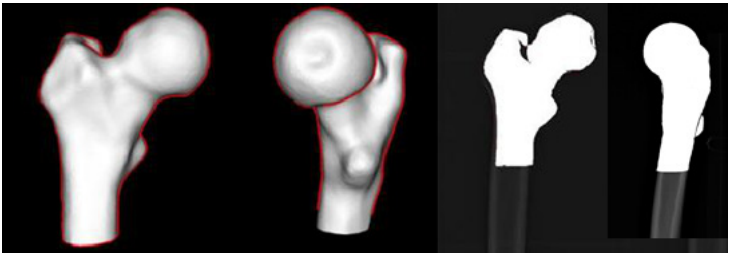

Figure 2: Sample results from the silhouette extraction scheme and generated masks.

3 Inferring the Model from Biplanar X-rays

Given a deformable model with the appropriate projective model for the low-dose system, we now define the metrics to quantify the discrepancy between the projected model and the biplanar X-rays. We define a specific objective function adapted for femoral modeling. The cost is based on a Geodesic Active Regions (GAR) framework [12]. The GAR functional is the convex combination of the geodesic active contours and geodesic active regions:

$$E_{GAR}(C_i(\mathbf{R},\mathbf{D})) = \alpha E_C(C_i(\mathbf{R},\mathbf{D})) + (1-\alpha)E_R(C_i(\mathbf{R},\mathbf{D})), \tag{3}$$

where C is the projected silhouette contours and α the weighting parameter. The active contours term reaches its minimum when the curve C falls along strong edges in the image, defining thus implicit distance maps defined as:

$$E_C(C_i(\mathbf{R},\mathbf{D})) = \oint_{C_i} g(C_i(s))ds \tag{4}$$

$$g(I) = \frac{1}{1+|\nabla I|}. \tag{5}$$

The geodesic active regions part is a log-likelihood objective function which aims to encapsulate femur-like pixels within the projected silhouette of the 3D model while excluding

background-like and other structure pixels:

$$E_R(C_i(\mathbf{R},\mathbf{D})) = -\int\int_R log(p_R(I_i(u,v)))dudv. \quad (6)$$

To apply this method to our problem, we must define a generative model which models the distribution of pixels intensities p_R inside the femoral region. Here, we adopt a nonparametric kernel density estimation method. Hence, this framework does not require any user interaction to define 2D contours on the X-ray images in order to match the ASM model to a segmented silhouette. Our method unifies segmentations in a coherent fashion with the registration problem.

3.1 Sequential rigid and deformable registration

The 2D/3D rigid registration consists in defining a geometric affine transformation defined by the parameter vector $\mathbf{R}$ that best specifies the position and orientation of the examined anatomy of the femur when acquiring the 2D projection images while dense registration consists of optimizing the ASM parameters defined by $\mathbf{D} = \{w_i\}_{i=1}^{L}$. In order to initialize the registration process, the approximate femoral head center in both images is identified. Since the projection matrices are known, it is possible to calculate the projection ray for any given image point. Thus, the 3D position of the femoral head midpoint can be easily found by a standard triangulation method using its 2D coordinates in order to align the imaging and world coordinate systems. To initialize the model given a set of biplanar X-ray images, we need to assess the quality of a candidate ASM instance, described by the parameter vector. This is done by measuring the most consistent ASM configuration for a new patient and the rigid parameter values corresponding to the minimal value of our cost function among possible parameter vectors is determined.

3.2 Optimization

As we formulate the inference as a minimization problem, we perform an iterative search to locate the parameters which obtains the minimum of the cost function. For each iteration of the algorithm, we use the current set of parameters to build the ASM model and simulate the observed X-ray images by the construction of binary silhouette images. We compute the quality of the consistence between these silhouette images and the corresponding X-ray acquisitions, followed by an update of the individual set of parameters until convergence is achieved so to obtain the optimal set. In order to identify in an efficient and/or reliable manner the set of updates, we need to define an optimization procedure which best suits the defined objective function. Gradient procedures use the gradient information to indicate the direction to the desired extremum. However, in our case, back-projection of the derivative of the objective function into the pose space is a complex procedure. Thus, we consider the Downhill simplex [8] method which is efficient in converging toward the desired minimum, requires only function evaluations and does not require the computation of derivatives. The following is the objective function which is to be minimized:

$$\mathbf{R},\mathbf{D} = \underset{\mathbf{R},\mathbf{D}}{\operatorname{argmin}}\, E_{GAR}(C_1(\mathbf{R},\mathbf{D})) + E_{GAR}(C_2(\mathbf{R},\mathbf{D})). \quad (7)$$

4 Synthetic and Clinical Experiments

4.1 Training data and methodological description

Our training database consists of 17 training surface models. The 17 training surface models were constructed from 17 binary volumes that were semi-automatically segmented from CT-datasets of patient hips. We use the first 10 principal modes of our PCA model, which statistically covers more than 99 % of the total variations of the model dataset.

Experiments were performed on both dry femurs and real clinical cases obtained from patients undergoing Total Knee Arthoplasty. We used 12 pairs of EOS images of a dry femur considered as our *in vitro* experiments, as well as 4 *in vivo* EOS images. We compared our results to those obtained by the gold standard CT segmented models as well as a method based on 2D manual segmentations. In order to estimate the error between the method and the ground truth, we compute the DICE coefficients and statistics anchored on point-to-surface distances. Moreover, clinicians, in the context of the Total Hip Replacement(THR) intervention, are interested in femur specific morphological parameters. The most important femur clinical parameters are the Neck Shaft Angle (NSA) and the Neck Shaft length (NSL) (Fig. 5). In order to estimate these parameters, we compute femur shaft axis and neck axis using the Scale Axis Transform method [2].

4.2 *In vitro* experiments

Ground-truth evaluation is performed on a set of available CT images. The error of the reconstructed model compared to CT was of 1.5 mm (Fig. 3, Table 1), which is in the range of acceptable tolerance for clinical assessment. We can observe from Fig. 3 that the maximum error is present in the the trochanter minor area. However shape variation in the trochanter area is fairly irrelevant for clinical purposes and therefore does not require for further processing. Surgeons are especially interested in the area of the femur head and neck. Our method exhibits excellent performance in these regions with respect to the manual method. In order to show that our method is able to achieve similar performance with the manual reconstruction method[7], despite the fact that our method is automatic, we compute point to surface distance to this supervised method (Table 2). Regarding the clinical parameters, statistics on error between the produced parameters and Ground Truth parameters are evaluated in Table 4

4.3 *In vivo* experiments

In order to avoid the problem of superposing contours which is critical in the sagittale image in the case of *in vivo* patients, we chose to work on images of patients oriented at 45° in the EOS cabin. For the *in vivo* validation with real clinical trials, at the absence of CT data, we computed the Hausdorff distance between manual 2D segmentations and our projected results on the X-ray images (Fig. 4, Table 3).

5 Discussion

While the SSM and the GAR were inspired from previous work, active shape/surface models were not considered within such an energy formulation, where the coefficients of the

Proposed method					Supervised method [7]			
Femur #	Mean	RMS	S.D.	DICE	Mean	RMS	S.D.	DICE
1	1.48	1.73	0.89	0.933	1.21	1.48	1.25	0.935
2	1.44	1.63	0.77	0.916	1.06	1.27	0.85	0.922
3	1.73	2.01	1.01	0.899	1.41	1.85	1.23	0.898
4	2.04	2.33	1.13	0.908	1.4	1.72	1.16	0.914
5	1.80	2.15	1.17	0.903	1.15	1.49	1.22	0.934

Table 1: Dice coefficients and point-to-surface distances (mm) to CT data.

Metrics					
Femur #	Min (mm)	Max (mm)	Mean (mm)	RMS (mm)	S.D. (mm)
1	0.03	8.72	1.73	2.18	1.34
2	0.04	8.16	1.8	2.3	1.33
3	0	8.16	1.8	2.3	1.33
4	0.09	7.3	1.46	1.83	1.09
5	0.04	9.84	1.86	2.34	1.42
6	0.1	9.82	1.91	2.3	1.29
7	0.05	10.3	1.82	2.48	1.69
8	0	10.05	1.64	2.15	1.38
9	0.01	5.44	1.36	1.64	0.97
10	0.03	8.02	2.11	2.59	1.6
11	0.06	7.06	2.12	2.57	1.51
12	0	7.45	1.65	2.02	1.31

Table 2: Point-to-surface distance compared to manual method.

Case#	Haussdorff distance (mm)
1	2.69
2	5.38
3	2.48
4	4.34

Table 3: Hausdorff distances to ground truth.

Error on	Neck Shaft Angle (degř)	Neck Shaft Length (mm)
Min	1.24	0.7
Max	4.16	3.9
Mean	2.26	1.84
S.D	0.78	0.64

Table 4: Errors on clinical parameters

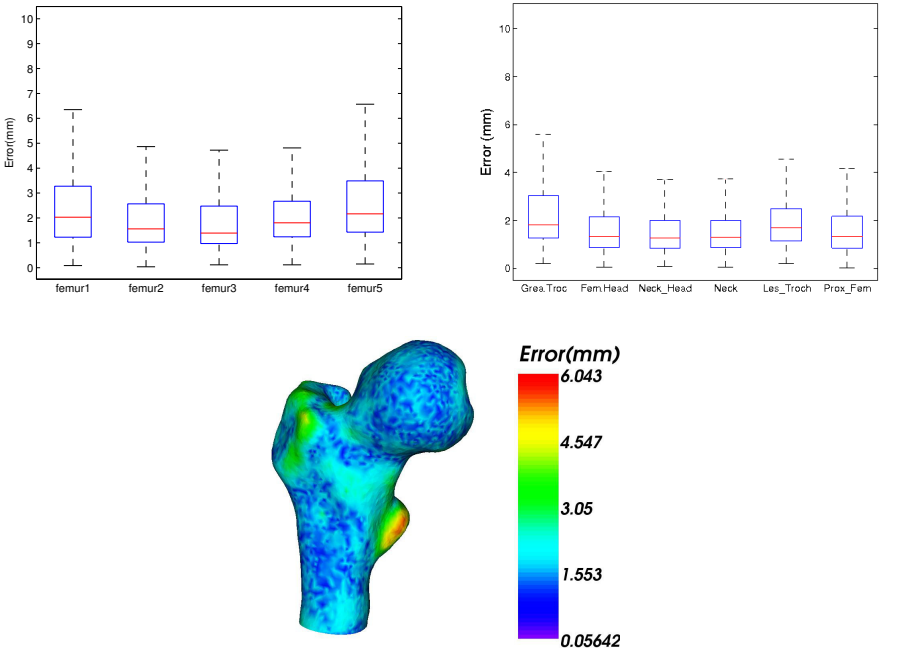

Figure 3: Point-to-surface distances to ground-truth CT models. Error distribution on mean femur model compared to CT.

subspace are estimated without explicit correspondences and one can infer 3D surface from 2D images. Conventional ASMs will fail in the context of this work since it is impossible to establish correspondences between the 3D model and the corresponding 2D projections. Moreover, opposite to conventional use of these models where optimal surface estimation is obtained through gradient descent on the parameter space, we consider a gradient free optimization method that allows to overcome the inverse projection of the gradient from the 2D images to the 3D space. Besides, Our automatic one-stage framework integrates a novel similarity metric adapted for femoral modeling, with implicit distance maps and intensity models to measure support from image data. Note that prior works proposed by [13] and [6] both of which need some manual interaction to determine 2D contours. Therefore, they require user intervention and a suitable user interface which is not practical in an inter-operative context.

Comparison with a supervised method was performed, in the experimental validation,to emphasize the novelty of our method. We show that our method is able to achieve similar performance with this manual reconstruction method[7], despite the fact that our method is automatic. Our data set could be improved, however we believe that preliminary results demonstrate the interest and the potentials of the method. Future work includes analyzing a larger data set.

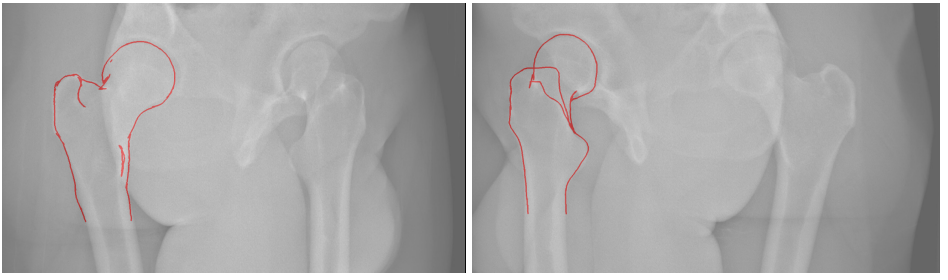

Figure 4: 2D segmentation results.

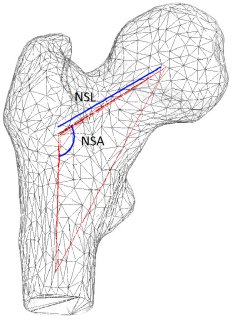

Figure 5: Schematic illustration of proximal Femur showing the axes for measurements of clinical parameters: Neck Shaft Angle (NSA) and Neck Shaft Length (NSL)

6 Conclusion

In this paper we have proposed a novel approach for femur pose estimation from biplanar X-ray images. The femur is represented using a triangulated surface topology where statistics are build from a linear sub-space. The parameters of this model are exploited along with the specific projection geometry of the EOS system to define an objective function that aims at separating the bone population from the background, while being primarily deformed towards from bone edges. Towards addressing the back-projection of the derivative of the objective function into the pose space, a gradient-free method is considered producing promising results. Future work includes analyzing a larger dataset of models and integrating the representation of the prior model using graphical models and the use of global pose-free parameters prior model and objective function. This can be achieved using higher order graphical models.

7 Acknowledgments

This work was supported by the European Research Council Starting Grant DIOCLES (ERC-STG-259112) and the MEDICEN Competitive Cluster sterEOS+ grant.

References

[1] T.F. Cootes, D. Cooper, C.J. Taylor, and J. Graham. Active Shape Models - Their Training and Application. *Computer Vision and Image Understanding*, 61:38–59, 1995.

[2] Joachim Giesen, Balint Miklos, Mark Pauly, and Camille Wormser. The scale axis transform. *ACM Symposium on Computational Geometry*, 2009.

[3] H. Gottschling, M. Roth, A. Schweikard, and R. Burgkart. Intraoperative fluoroscopy-based planning for complex osteotomies of the proximal femur. *Int J Med Robotics Comput Assist Surg*, 2005.

[4] T. Heimann and H.-P. Meinzer. Statistical shape models for 3D medical image segmentation: A review. *Medical Image Analysis*, 13:543–563, 2009.

[5] S. Kadoury, F. Cheriet, F. Laporte, and H. Labelle. A versatile 3D reconstruction system of the spine and pelvis for clinical assessment of spinal deformities. *Medical and Biological Engineering and Computing*, pages 591–602, 2007.

[6] R. Kurazume, K. Kaori Nakamuraa, T Okadab, Y Satoc, N Suganoc, T Koyamad, Y Iwashitaa, and T Hasegawaa. 3D reconstruction of a femoral shape using a parametric model and two 2D fluoroscopic images. *Computer Vision and Image Understanding*, 113:202–211, 2009.

[7] S. Laporte, J. Skalli, W.and de Guise , F. Lavaste, and D. Mitton. A Biplanar Reconstruction Method Based on 2D and 3D Contours: Application to the Distal Femur. *Computer Methods in Biomechanics and Biomedical Engineering*, 6:1–6, 2003.

[8] R. Lewis, A. Shepherd, and V. Torczon. Implementing generating set search methods for linearly constrained minimization. *SIAM J. Sci. Comput.*, 6:2507–2530, 2007.

[9] D. Mitton, S. Deschênes, S. Laporte, B. Godbout, S. Bertrand, J. A. de Guise, and W. Skalli. 3D reconstruction of the pelvis from bi-planar radiography. *Computer methods in biomechanics and biomedical engineering*, pages 1–5, 2006.

[10] T Tang and R. Ellis. 2D/3D Deformable Registration Using a Hybrid Atlas. *MICCAI*, 3750/2005:223–230, 2005.

[11] JP. Thirion. Image matching as a diffusion processs: an analogy with MaxwellŠs demons. *Med Image Anal*, 2:243–260, 1998.

[12] K. Varshney, N. Paragios, A. Kulski, R. Raymond, P. Hernigou, and A. Rahmouni. Post-Arthroplasty Examination Using X-Ray Images. *IEEE Transactions on Medical Imaging*, 28:469–474, 2009.

[13] G. Zheng and S. Schumann. 3D reconstruction of a patient-specific surface model of the proximal femur from calibrated x-ray radiographs: a validation study. *Medical Physics*, pages 1155–1166, 2009.